Contents

Chapter 1

Theory

1.1 Higgs Phenomenology

The Higgs sector of the Minimal Supersymmetric Standard Model (MSSM) consists of two SU (2) dou- blets, H1 and H2 , whose relative contribution to electroweak symmetry breaking is determined by the ratio of vacuum expectation values of their neutral components, tan v2 /v1 . The spectrum of phys- ical Higgs bosons is richer than in the SM, consisting of two neutral scalars h and H, one neutral pseu- doscalar, A, and two charged scalars, H. At the tree level, the mass matrix for the neutral scalars can be expressed in terms of the parameters MZ , MA and tan , and the mass of the lightest scalar h is bounded from above by MZ . However, radiative corrections especially those involving top and bottom quarks and their supersymmetric partners, the stop and sbottom squarks can significantly alter the tree-level predictions for the Higgs-boson masses, and bring along a dependence on a large number of free pa- rameters of the MSSM. While the CP symmetry is conserved at tree level in the MSSM Higgs sector, radiative corrections can also introduce CP-violating phases, and induce mixing among all three neutral states. In this report, however, we will focus on the CP-conserving case, by considering only real values for the parameters in the soft SUSY-breaking Lagrangian and for the Higgs mass in the superpotential. In general, the couplings of the MSSM Higgs bosons to gauge bosons and matter fermions dif- fer from those of the SM Higgs. However, in large regions of the MSSM parameter space one of the scalars has SM-like couplings, while the other Higgs bosons are decoupled from the gauge bosons, and their couplings to down-type (up-type) fermions are enhanced (suppressed) by tan . As in the SM, gluon fusion is one of the most important production mechanisms for the neutral Higgs bosons, whose couplings to the gluons are mediated by the top and bottom quarks and their superpartners. However, for intermediate to large values of tan the associated production with bottom quarks can become the dominant production mechanism for the neutral Higgs bosons that have enhanced couplings to down- type fermions. The production of the charged Higgs H, on the other hand, proceeds mainly through its coupling to a top-bottom pair. A sufficiently light H is produced in the decay of a top quark, and it decays dominantly in a tau-neutrino pair. A heavy H is produced in association with a top quark and it decays dominantly in a top-bottom pair. The discovery by ATLAS and CMS of

what appears to be a neutral scalar with mass around 125.5 GeV [1, 2] puts the studies of the Higgs sector of the MSSM in an entirely new perspective. In order to remain viable, a point in the MSSM parameter space must now not only pass all the (ever stricter) experimental bounds on superparticle masses, but also lead to the prediction of a scalar with mass, production cross section and decay rates compatible with those measured at the LHC. In particular, the relatively large mass of the roughly-SM-like scalar discovered at the LHC implies either very heavy stops, of the order of 3 TeV, or a large value of the left-right stop mixing term (see, e.g., Refs. [648,649]). The benchmark scenarios routinely considered in MSSM studies had been devised when the Higgs sector was constrained only by the LEP searches, and many of them, such as the so-called no-mixing scenario, are now ruled out because they predict a too-light SM-like scalar. Others, such as the so-called mmax scenario, are constrained for the opposite reason, i.e. they can predict a too-heavy SM-like scalar. h To address the need for new benchmark scenarios to be used in future studies of the MSSM Higgs sector, in Section 14.2 we will define scenarios that are compatible both with the properties of the Higgs boson discovered at the LHC and with the current bounds on superparticle masses. The fact that information on the Higgs boson mass, production and decays has now become avail- able also puts new emphasis on the need for accurate theoretical predictions of those quantities. In the studies presented in this report, the masses and mixing of the MSSM Higgs bosons are computed with the public code F EYN H IGGS [2427], which implements the full one-loop radiative corrections together with the dominant two-loop effects. The theoretical accuracy of the prediction of F EYN H IGGS for the

lightest-scalar mass was estimated to be of the order of 3 GeV [26, 650, 651], i.e., already comparable to the accuracy of the mass measurement at the LHC. Improving the accuracy of the theoretical predic- tion for the MSSM Higgs masses will require the inclusion in public computer codes of the remaining two-loop effects [652654] and at least the dominant three-loop effects [655657]. The production and decay rates of a SM-like Higgs boson in the MSSM are sensitive to contributions from virtual SUSY particles, and their measurement at the LHC combined with the searches for additional Higgs bosons can be used to constrain the MSSM parameter space. To this effect, the theoretical predictions for cross section and decays must include precise computations of the SUSY con- tributions. In Section 14.3 we use the public code S US H I [641] and the POWHEG implementation of Ref. [77] to compute the total and differential cross sections for neutral Higgs-boson production in gluon fusion, including a NLO-QCD calculation of quark and squark contributions plus higher-order quark contributions adapted from the SM calculation. We show that the SUSY contributions can be sizeable in regions of the MSSM parameter space where the third-generation squarks are relatively light, and discuss the theoretical uncertainty of the predictions for the cross sections. Finally, we study and update the exclusion limits on light charged MSSM Higgs bosons in the (MH , tan)-plane in various benchmark scenarios in Section 14.4. Particular emphasis is placed on the dependence of the limits on the variation of SUSY parameters. We also provide improved NLO- QCD cross section predictions for heavy charged Higgs production in the so-called four and five-flavor schemes in Section 14.5. The five-flavor scheme cross section is calculated with a new scheme

for setting the factorization scale and takes into account the theoretical uncertainty from scale variation and the PDF, s and bottom-mass error. We observe good agreement between the 4FS and 5FS NLO-calculations and provide a combined prediction following the Santander matching. 14.2 New MSSM benchmark scenarios Within the MSSM an obvious possibility is to interpret the new state at about 125.5 GeV as the light CP-even Higgs boson [334, 338, 648, 649, 658662]. At the same time, the search for the other Higgs bosons has continued. The non-observation of any additional state in the other Higgs search channels puts by now stringent constraints on the MSSM parameter space, in particular on the values of the tree- level parameters MA (or MH) and tan . Similarly, the non-observation of supersymmetric (SUSY) particles puts relevant constraints on the masses of the first and second generation scalar quarks and the gluino, and to lesser degree on the stop and sbottom masses (see Refs. [663, 664] for a recent summary). Due to the large number of free parameters, a complete scan of the MSSM parameter space is impractical in experimental analyses and phenomenological studies. Therefore, the Higgs search results at LEP were interpreted [458] in several benchmark scenarios [16, 665]. In these scenarios only the two parameters that enter the Higgs sector tree-level predictions, MA and tan , are varied (and the results are usually displayed in the MA tan plane), whereas the other SUSY parameters, entering via radiative corrections, are fixed to particular benchmark values which are chosen to exhibit certain features of the MSSM Higgs phenomenology. These scenarios were also employed for the MSSM Higgs searches at the Tevatron and at the LHC. By now, most of the parameter space of the original benchmark scenarios [16, 665] has been ruled out by the requirement that one of the CP-even Higgs boson masses should be around 125.5 GeV. Consequently, new scenarios have been proposed [31], which are defined such that over large parts of their available parameter space the observed signal at about 125.5 GeV can be interpreted in terms of one of the (neutral) Higgs bosons, while the scenarios exhibit interesting phenomenology for the MSSM Higgs sector. The benchmark scenarios are all specified using low-energy MSSM parameters, i.e. no particular soft SUSY-breaking scenario was assumed. Constraints from direct searches for Higgs bosons are taken into account, whereas indirect constraints from requiring the correct cold dark matter density, BR(b s), BR(Bs +) or (g2) are neglected. However interesting, those constraints de

Chapter 2

The Search for neutral MSSM Higgs Bosons in the final state: $\tau^+\tau^- \to e\mu + 4\nu$

This chapter contain the main work of this thesis, reports about the search the neutral MSSM Higgs bonon decaying in tau pairs and fully leptonic final state. This search is based on 2012 8 TeV data recorded by ATLAS experiment at Large Hadron Collider.

Discovering the mechanism responsible for electroweak symmetry-breaking and the origin of mass for elementary particles has been one of the major goals of the physics program at the Large Hadron Collider (LHC) [1]. In the Standard Model (SM) this mechanism requires the existence of a single scalar particle, the Higgs boson [2, 3, 4, 5, 6]. In the Minimal Supersymmetric extension of the Standard Model (MSSM) [7, 8] the Higgs sector is composed of two Higgs doublets of opposite hyper-charge, resulting in five observable Higgs bosons. Two of these Higgs bosons are neutral and CP-even (h,H), one is neutral and CP-odd (A) and two are charged ($H^{\pm}$). At tree level their properties such as masses, widths and branching ratios can be predicted in terms of only two parameters, often chosen to be the mass of the CP-odd Higgs boson m_A, and the ratio of the vacuum expectation values of the two Higgs doublets $\tan\beta$ (more detail in chapter **??**).

This chapter is divided in three sections: in section 2.1 an introduction to experimental searches and to the strategy of this particular analysis is given, in section **??** is described the core of this thesis work, i.e. the detail of the background modeling for this analysis, while in section **??** the result of the sarch are presented.

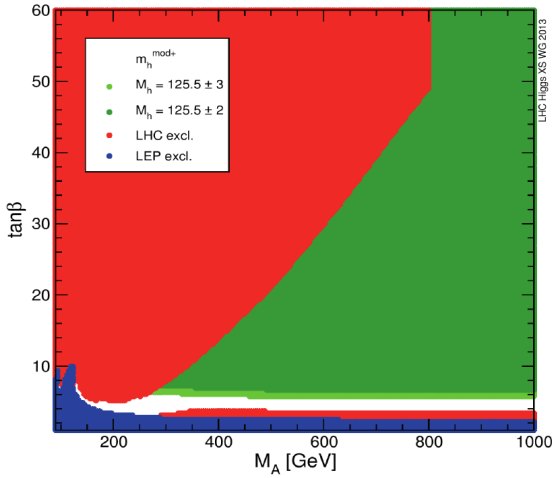

Figure 2.1: $m_A - \tan\beta$ plane for the m_h^{mod+} scenario, with excluded region from direct Higgs searches at Lep (blue) and LHC (red). The two green shades corresponds to the allowed parameter space for the assumption of $M_h = 125.5 \pm 2(3)$ GeV. For more detail see [].

2.1 The Search Strategy

2.1.1 Motivation

Under the light of the recent discovery of a Higgs boson with mass of 125 GeV [], remains an open question wheter this new particle constitute all the pieces of the Higgs sector or if it is only one of several bosons predicted in some theories that go beyond the SM. The most recent measurements [] of its properties shows it to be, within experimental uncertainties, perfectly compatible with the SM Higgs boson, however such a new particle can be accomodated within several beyond the standard model (BSM) theories, this is particularly true for Super Symmetry.

There are two approach to explore the Higgs sector: studying the cupling of the Higgs boson with vector bosons and fermions, given the unitarity property of scattering aplitudes for longitudinal vectors and fermions, one can understand if this particle is fully responsible for the generation of the masses of all the other SM particles. Another approach is to directly search for for additional Higgses in a well defined model. In this thesis the last approach is followed, new particle are sought within the MSSM scenario (see chapter **??**).

In the MSSM a Higgs boson with properties that resembles the one for a SM Higgs boson occures naturally in large regions of parameter space, for practical reason however, is usefull to fix parameter of the model to achieve what is called a benchmark scenario. With the recenty discovery, bechmark scenario of the MSSM have been updated to fit with the new constraints (more details on benchmark scenarios are in chapter **??**), as an example in figure **??** are reported the current exclusion limits for one of those updated scenarios, m_h^{mod+}, the green area represents what is currently allowed in the $m_A - \tan\beta$ plane showing that there is still plenty of room for BSM Higges.

2.1.2 How to search for new phenomena?

Typically new physics searches are looking for a signal that is additive on top of the background, an observation of an excess or exclusion of a signal is then characterize by statistical statemetnts. A *statistical test* is a rule used to reject or accept an hypotesis. An hypotesis is a statement about the distribution of the data. In the search for new phenomena at the LHC frequentistic statistical tests are used [**?**], where two hypotesis are compared: the background only hypotesis H_0, which plays the role of the null hypotesis, and the signal plus background hypotesis H_1, which is the alternative. In this section an itroduction to LHC statistical procedure is given, for more details see section **??**.

In a search for new physics usually a *signal region* is defined in data where events are counted, the number of observed events N_{SR} is a random variable described by a Poisson distribution, in case the null hypotesis is true ν_B events are expected, while $\nu_B+\nu_S$ are expected for the H_1 alternative hyspotesis, the probability model for null and the alternate hypotesis is ithen respectively Pois$(N_{SR}|\nu_B)$ and Pois$(N_{SR}|\nu_B + \nu_S)$. The evidence for a signal shows up as an excess of events, a way to quantify the conpatibility of the null hypotesis with data is to make a *significance* test, this leads to the calculation of the probability that the background-only would produce at least as many as the observed events, this is the so called of p-value, which in this case is expressed by the formula:

$$\text{p-value} = \sum_{n=N_{SR}}^{\infty} \text{Pois}(n|\nu_B)$$

Calculating p-value is a way to characterize an excess, in high energy physics the commonly accepted p-value that qualifies as discovery is 2.87×10^{-7}, which translated to the probability of a gaussian distribution correspond to five standard deviation.

In case no excess is observed, the procedure is to build a statisctical test where the null hypotesis is accepted and at the same time the signal hypotesis is rejected with a fixed predetermined probability, called confidence level. A statistical test is a rule that defines a region in the space of data for which a given hypotesis can be accepted or rejected, often rather than using a full set of data $\mathcal{D}$, it is convenient to define a *test statistic*, T, which is usually a single number computed from the data, the two hypotesis implies different distributions for T, then one defines an acceptance region W in terms of the test statistic, if $T \in W$ the H_0 is rejected and H_1 accepted and vice versa, the probability with which one rejects H_1 or H_0 is then given by the choice of W and T. Neuman and Person provided a framework for hypotesis testing that addresses the choice of the test statistic [**?**].

A discriminating variable is often used to help separating signal and backgrounds, this can be any of the observables of the experiment, a usually chosen observable is for example the invariant mass of final state particles, knowing the probability density function $f(x)$ for this observable for the two hypotesis one can complete the above mentioned statistical model with what is called a marked Pois-

son for a set of data $\mathcal{D}$:

$$\text{Pois}(N_{SR}|\nu)\prod_{i\in\mathcal{D}}^{N_{SR}} f(x_i|\vec{\theta})$$

here is made explicit that $f(x)$ depends also on a set of additional parameter $\vec{\theta}$, called nuissance parameter, those embed effects like detector mismodeling or theoretical uncertainty. With the use of a discriminating variable one can take advantage of additional information to disentangle between signal and backgrounds.

Summarizing, there are several ingredients that constitute a search for new physics and will be discussed with more details in the following sections:

- Define a signal region in data where signal is enhanced with respect to the backgrounds, detailed in section **??**
- Define a discriminating variable which is usefull to disentangle between signal and backgrounds, section **??**
- Define the probability model, i.e., the expectation for the distribution of the discriminating variable for signal and background hypotesis, this is one of the most importat point of a search and main part of the work of this thesis, detailed in section **??**
- Define a test statistics, which is detailed for the LHC in section **??**.

2.1.3 Signal Topology

This section describes the strategy to enhance the search sensitivity taking advantage of the signal topology. The Sensitivity of a search is the signal strenght that is expected to be excluded in case of no signal. If one is searching for a rare process, then the analysis strategy, i.e. the plan or the steps to enhance the signal sensitivity of the search, is crucial. A further consideration is that this search is complementary to the Standard Model Higgs search in tau final state, the focus is then on non explored phase space from SM.

In the MSSM for large region of parameter space one found that one of the CP-even neutral Higgses is has properties that resemble the one of the SM Higgs, this is usually the case for the lightest Higgs, h, the other two, H and A, thend to be degenerate in mass and decouple from gauge bosons. An interesting fenomenological point is that the coupling of the latter two Higgses with down (up) type fermions are enhanced (suppressed) by $\tan\beta$, meaning that for large $\tan\beta$ bottom-quark and τ lepton will play a more important role than in the SM case either for production and decay.

The production of the neutral CP-even MSSM Higgs bosons at hadron colliders proceeds via the same processes as for the SM Higgs production. However, the pseudoscalar A instead cannot be produced in association with gauge bosons or in vector boson fusion (VBF) at tree-level, as this coupling is forbidden due to CP-invariance. At the LHC one of the most relevant production mechanisms for the MSSM Higgs bosons is gluon-gluon fusion, $gg \to A/H/h$. In addition, the

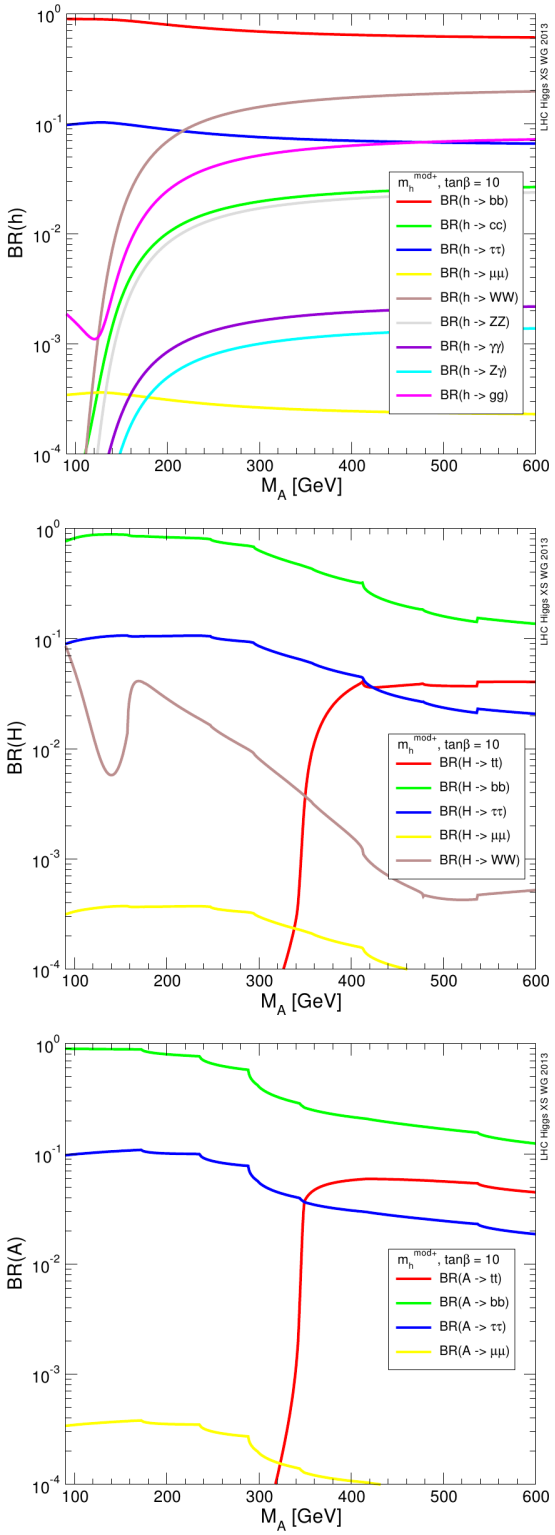

Figure 2.2: Branching fraction for the MSSM neutral higgses in the bla scenario.

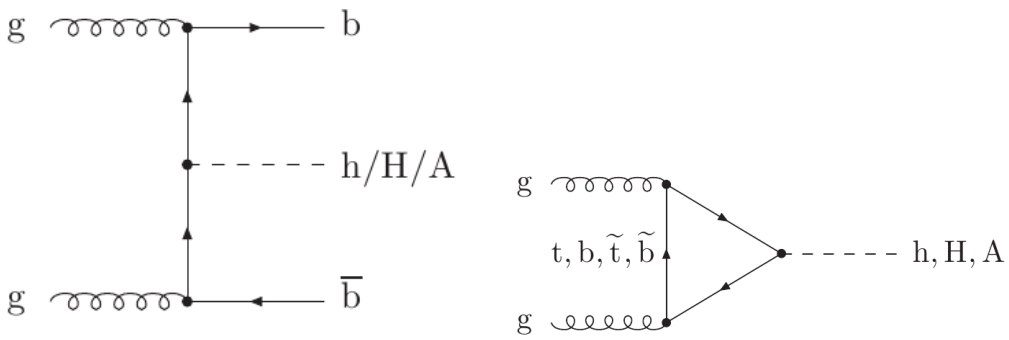

Figure 2.3: Diagram for b-associated production and gluon-gluon fusion for MSSM neutral Higgs.

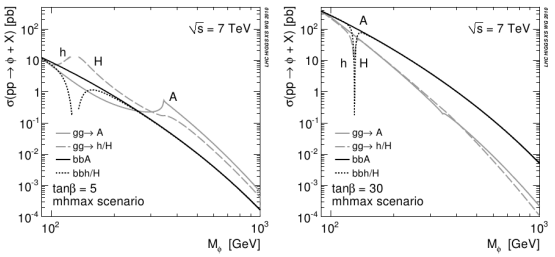

Figure 2.4: Cross section for different MSSM neutral Higgs production mode.

production in association with b-quarks becomes important for large value of $\tan\beta$. Those are the two production mechanism that are considered in this analysis, figure **??** shows the feyinman-diagram for those processes. The search is divided in two category which are optimized for the two different production mode considered, in the gluon-fusion category is requred a b-jet veto, in fact no b-jet in the final state are present for this production mode. In contrast a a b-jet tag is required for b-associated production, this category is expected to be very sensitive to $\tan\beta$. The two category are ortogonal and present different backgrounds contributions, which can be optimized separately.

The decays of the neutral MSSM Higgs bosons (in the assumption that all supersymmetric particle are heavy enough) are the same as for the SM one with the already cited exception of A. Figure **??** shows the decay branching fractions for H and A, as a function of the mass and for $\tan\beta =$, the decay into tau pair is the most important after $b\bar{b}$. The decay channel in $b\bar{b}$ is challenging due to the huge background from QCD multi-jet, in this analysis the decay in tau pairs is choosen. In this thesis only cases in which the taus decay one in $e + 2\nu$ and the other in $\mu + 2\nu$ are considered, This final state corresponds to a total $\tau^+\tau^-$ branching ratio of approximately 6%.

Summarising, the signal topology is characterised by a final state with an electron, a muon, and missing transverse energy due to the presence of four neutrinos from the τ decays. Furthermore, the final state may be split by the presence or absence of a b-quark initiated jet, depending on the production process. This signature is achieved experimentally by requiring: an OR of a single elecron and an electron-muon trigger, exactly one reconstructed electron and one muon in the final state, the two leptons should be of opposite charge and isolated. With isolation it's meant that in a cone around the lepton there should be little energy deposit (should not be sorraunded by other particle, common of non-promt leptons coming from jets). More detail about isolation properties are detailed in section **??**. Full detail on actual preselections regarding all the quality requirements on object reconstruction are reported in appendix **??**.

2.1.4 How to deal with Backgrounds

The signal topology described in the previous section common to many other processes, unfortunately those have higher cross section than the signal we are looking for, a set of additional selection has been studied to enhance the sensitivity of the search, or in other words, to increase the signal to background ratio. The most important backgrounds to this search are the production of $Z \to \tau\tau$ + jets, the top quark ($t\bar{t}$ and single top production is intended), diboson production (like WW or ZZ events) and events with non-prompt leptons coming from QCD multi-jet (in short QCD multi-jet). Vector bosons production like $W \to l\nu$ or $Z \to ll$ + jets (with l here meanung either e or μ) are also considered, however those processes have a limited impact.

The final state of Higgs decaying into tau pair coincide with the one from $Z \to \tau\tau$ process, this is then an irreducible background, however exploiting the different kinematics of the Higgs decay and the other backgrounds it possible to distinguish

between signal and them. The most stiking is that the higgs (like $Z \to \tau\tau$) selecting an electron and one muon coming from the tau decay, due to the high mass the taus will be back to back and their decay products will be highly boosted, this gives rise to two feature: the mu-e will be more likely back to back, as you can see in figure 2.5 that shows the angle between the leptons in the transverse plane $\Delta\phi = |\phi_e - \phi_\mu|$[1] prefer configuration in wich the leptons are in opposite emisphere. Furthermore the neutrinos will be more likely collinear with the leptons (given the high boost the taus recive from Higgs decay). This feature can be matematically seen as the sum of scalar product between missing energy and the leptons four-vectors in the transverse plane, if the vectors are normalised to unit versors then what remains is a relation only between angles:

$$\hat{E}_T^{miss} \cdot (\hat{P}_T^{\mu} + \hat{P}_T^{e}) = cos(\Delta\phi_{E_T,\mu}) + cos(\Delta\phi_{E_T,e})$$

In the assuption of collinearity and of leptons back-to-back that scalar product is equal to zero, in fact it would be equal to zero for each of the neutrinos being it collinear with one lepton and back-to-back with the other. As can be seen from figure 2.5 in fact the distribution of that variable has its more likely values at zero. These two feature can be used to distinguish between mu-e coming from decay from highly boosted object and the one coming from W decays in top or in dibosons backgrounds which will have a more spread distribution. In b-veto category these two selections are sufficient to suppress contribution from dibosons, no other selection is applied in this category because it has been shown to not bring significant improvement.

In the b-tag category the situation is different, the request of b-jet enhance backgrounds with high jet activity as top production, given the relatively low jet activity of our Higgs events (also in the case of b-associated production) it's possible to separate them from top production which instead is very likely to have 2 or more highly enegetic jets in the event, requesting a small jet activity, this is achieved by requesting the sum of the jets transverse momentum to be small, we call this variable H_T. Another feature that distinguish top pair production from Higgs is the much higher invariant mass of the former final state, in the transverse plane all the leptons will tend to have a higher momentum, we then use the sum of lepton p_t and E_T^{miss} as a discriminating variable, requesting it to be small. Figure **??** shows the distribution of these two variables after the request of a b-jet.

Plots with MMC mass as a function of selection that shows how effective they are in reducing backgrounds.

In table **??** a summary of all the selection variable used with their optimized cut values is reported. While in table **??** the number of events that survises at each cut stage for different background is reported.

2.1.5 Missing Mass Calculator

Accurate invariant mass reconstruction of a di-tau system is a challenging task due to the escaping neutrinos. In this analysis, with four neutrinos in the final state,

[1]This is actually more complicated: one has to take care of the sign of ϕ see chapter**??**

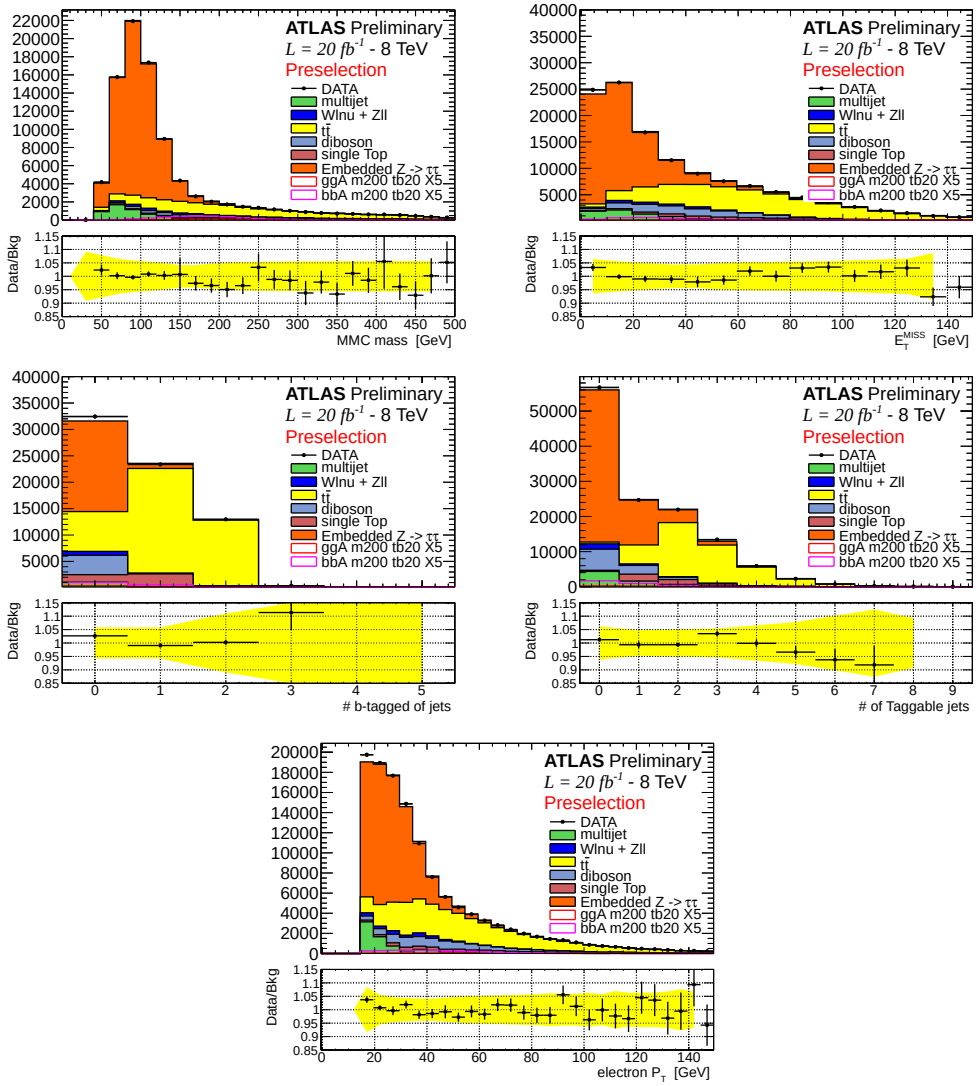

Figure 2.5: bla

the number of unknown largely exceed the number of constraints, several approximation are possible to further constraint the neutrinos, for example assuming them collinear to the other leptons from tau decay, however those approximation suffers of limitations.

In this analysis we use the so called missing mass calculator (MMC) [55] technique for the calculation of the di-tau system invariant mass. This technique employs additional information from the well known tau decay to constraint the system, this is achieved by minimising a likelihood function defined in the kinematically allowed phase space region, the result is a more precise measurement of the di-tau system invariant mass and a considerable improvement in resolution. The invariant mass distribution calculated with the MMC technique is referred in the following as MMC_{mass} and is used as discriminating variable in the limits setting.

2.2 Background Modeling

In this section we make use of analysis tools described in chapter **??**, as well we refer to objetc definition made in this chapter (like electron reconstruction, jet difinition, muons, ecc.).

2.2.1 MC samples

2.2.2 Embedding

2.2.3 ABCD Method for QCD

2.2.4 Top validation

2.2.5 Systematics

2.3 Results

2.3.1 Statistics

2.3.2 Exclusion Limits

2.3.3 Summary

Bibliography

[1] L. Evans and P. Bryant, *LHC Machine*, JINST **3** (2008) S08001.

[2] F. Englert and R. Brout, *Broken Symmetry and the Mass of Gauge Vector Mesons*, Phys. Rev. Lett. **13** (1964) 321.

[3] P. W. Higgs, *Broken symmetries, massless particles and gauge fields*, Phys. Lett. **12** (1964) 132.

[4] P. W. Higgs, *Broken Symmetries and the Masses of Gauge Bosons*, Phys. Rev. Lett. **13** (1964) 508.

[5] P. W. Higgs, *Spontaneous Symmetry Breakdown without Massless Bosons*, Phys. Rev. **145** (1966) 1156.

[6] G. S. Guralnik, C.R. Hagen and T. W. B. Kibble Phys.Rev.Lett. **13** (1964) 585.

[7] N. P. Nilles, *Supersymmetry, supergravity and particle physics*, Phys. Rep. **110** (1984) 1.

[8] H. E. Haber and G. L. Kane, *The search for supersymmetry: Probing physics beyond the standard model*, Phys. Rep. **117** (1985) 75.

[9] ALEPH, DELPHI, L3 and OPAL Collaboration, *Search for neutral MSSM Higgs bosons at LEP*, Eur. Phys. J. **C47** (2006) 547.

[10] *Combined CDF and D0 upper limits on MSSM Higgs boson production in tau-tau final states with up to 2.2 fb^{-1} of data*, `arXiv:1003.3363 [hep-ex]`.

[11] CDF Collaboration, T. Aaltonen et al. Phys. Rev. Lett. **103** (2009) 201801.

[12] D0 Collaboration, V. Abazov et al. Phys. Rev. Lett. **101** (2008) 071804.

[13] TNPWG (Tevatron New Physics Higgs Working Group), CDF and D0 Collaborations, *Search for Neutral Higgs Bosons in Events with Multiple Bottom Quarks at the Tevatron*, `arXiv:1207.2757 [hep-ex]`.

[14] CDF Collaboration, T. Aaltonen et al., *Search for Higgs Bosons Produced in Association with b-quarks*, Phys.Rev. **D85** (2012) 032005, `arXiv:1106.4782 [hep-ex]`.

[15] D0 Collaboration, V.M. Abazov et al., *Search for neutral Higgs bosons in the multi-b-jet topology in 5.2fb^{-1} of $p\bar{p}$ collisions at $\sqrt{s} = 1.96$ TeV*, Phys.Lett. **B698** (2011) 97–104, arXiv:1011.1931 [hep-ex].

[16] The CMS Collaboration, S. Chatrchyan et al., arXiv:1104.1619 [hep-ex] [hep-ex].

[17] The ATLAS Collaboration , *Search for the neutral Higgs bosons of the Minimal Supersymmetric Standard Model in pp collisions at $\sqrt{s} = 7$ TeV with the ATLAS detector*, arXiv:1211.6956 [hep-ex].

[18] T. A. Collaboration, *Observation of a new particle in the search for the Standard Model Higgs boson with the ATLAS detector at the LHC*, Physics Letters B **716** (2012) 1–29.

[19] T. C. Collatoration, *Observation of a new boson at a mass of 125 GeV with the CMS experiment at the LHC*, Physics Letters B **716** (2012) 30–61.

[20] S. Heinemeyer, O. Stål and G. Weiglein, *Interpreting the LHC Higgs search results in the MSSM*, Phys.Lett. **B710** (2012) 201–206, arXiv:1112.3026 [hep-ph].

[21] A. Arbey, M. Battaglia, A. Djouadi and F. Mahmoudi, *The Higgs sector of the phenomenological MSSM in the light of the Higgs boson discovery*, JHEP **1209** (2012) 107, arXiv:1207.1348 [hep-ph].

[22] The ATLAS Collaboration, G. Aad et al., *The ATLAS Experiment at the CERN Large Hadron Collider*, JINST **3** (2008) S08003.

[23] M. L. Mangano et al., *ALPGEN, a generator for hard multiparton processes in hadronic collisions*, JHEP **07** (2003) 001.

[24] J. Alwall et al., *Comparative study of various algorithms for the merging of parton showers and matrix elements in hadronic collisions*, Eur. Phys. J. **C53** (2008) 473, arXiv:0706.2569.

[25] S. Frixione and B. R. Webber, *Matching NLO QCD computations and parton shower simulations*, JHEP **06** (2002) 029, hep-ph/0204244.

[26] B. P. Kersevan and E. Richter-Was, *The Monte Carlo Event Generator AcerMC 2.0 with Interfaces to PYTHIA 6.2 and HERWIG 6.5*, arXiv:0405247v1 [hep-ph].

[27] G. Corcella et al., *HERWIG 6: an event generator for hadron emission reactions with interfering gluons (including supersymmetric processes)*, JHEP **01** (2001) 010.

[28] J. M. Butterworth, J. R. Forshaw, and M. H. Seymour, *Multiparton Interactions in Photoproduction at HERA*, Z. Phys. **C72** (1996) 637.

[29] T. Binoth, M. Ciccolini, N. Kauer, and M. Kramer, *Gluon-induced W-boson pair production at the LHC*, JHEP **12** (2006) 046.

[30] A. S. et al., *Higgs boson production in gluon fusion*, JHEP **02** (2009) 029.

[31] T. Gleisberg et al., *Event generation with SHERPA 1.1*, JHEP **02** (2009) 007.

[32] J. Pumplin, D. R. Stump, J. Huston, H. L. Lai, P. M. Nadolsky and W. K. Tung, "New generation of parton distributions with uncertainties from global QCD analysis," JHEP **0207** (2002) 012 [hep-ph/0201195].

[33] H. -L. Lai, M. Guzzi, J. Huston, Z. Li, P. M. Nadolsky, J. Pumplin and C. -P. Yuan, "New parton distributions for collider physics," Phys. Rev. D **82** (2010) 074024 [arXiv:1007.2241 [hep-ph]].

[34] M. Carena, S. Heinemeyer, C. E. M. Wagner, and G. Weiglein, *Suggestions for benchmark scenarios for MSSM Higgs boson searches at hadron colliders*, Eur. Phys. J. **C26** (2003) 601–607, `hep-ph/0202167`.

[35] The ATLAS Collaboration, *ATLAS Monte Carlo Tunes for MC09*, ATL-PHYS-PUB-2010-002.

[36] S. Jadach, J. H. Kuhn and Z. Was, *TAUOLA - a library of Monte Carlo programs to simulate decays of polarized τ leptons*, Comput. Phys. Commun. **64** (1990) 275.

[37] E. Barberio, B. V. Eijk and Z. Was, *Photos - a universal Monte Carlo for QED radiative corrections in decays*, Comput. Phys. Commun. **66** (1991) 115.

[38] The GEANT4 Collaboration, S. Agostinelli et al., *GEANT4 - a simulation toolkit*, Nucl. Instrum. Meth. **A506** (2003) 250.

[39] The ATLAS Collaboration, G. Aad et al., *The ATLAS Simulation Infrastructure*, ATLAS-SOFT-2010-01-004, submitted to Eur. Phys. J. C., `arXiv:1005.4568`.

[40] The ATLAS Collaboration, *Estimation of $Z \to \tau\tau$ Background in VBF $H \to \tau\tau$ Searches from $Z \to \mu\mu$ Data using an Embedding Technique*, ATL-PHYS-INT-2009-109.

[41] The ATLAS Collaboration, *Search for the Standard Model Higgs boson in the $H \to \tau\tau$ decay mode with 4.7 f b1 of ATLAS detactor*, Tech. Rep. ATLAS-CONF-2012-014, CERN, Geneva, Mar, 2012.

[42] The ATLAS Collaboration, *Search for the Standard Model Higgs boson $H \to \tau\tau$ decays with the ATLAS detector*, ATL-COM-PHYS-2013-722.

[43] T. S. et al., Z *physics at LEP 1*, CERN 89-08 **3** (1989) 143.

[44] The ATLAS Collaboration, *Expected Performance of the ATLAS Experiment - Detector, Trigger and Physics*, CERN-OPEN-2008-020, `arXiv:0901.0512`.

[45] The ATLAS Collaboration, *ATLAS Muon Momentum Resolution in the First Pass Reconstruction of the 2010 p-p Collision Data at* $\sqrt{s} = 7$ *TeV*, ATLAS-CONF-2011-046.

[46] The ATLAS Collaboration, *Muon reconstruction efficiency in reprocessed 2010 LHC p-p collision data recorded with the ATLAS detector*, ATLAS-CONF-2011-063.

[47] The ATLAS Collaboration, *Expected electron performance in the ATLAS experiment*, ATLAS-PUB-2011-006.

[48] ATLAS egamma WG, *Electron efficiency measurements*, https://twiki.cern.ch/twiki/bin/view/AtlasProtected/EfficiencyMeasurements.

[49] M. Cacciari, G. P. Salam, and G. Soyez, *The anti-k_t jet clustering algorithm*, JHEP **04** (2008) 063.

[50] W. Lampl et al., *Calorimeter Clustering Algorithms : Description and Performance*, ATL-LARG-PUB-2008-002.

[51] T. Barillari et al., *Local Hadron Calibration*, ATL-LARG-PUB-2009-001.

[52] The ATLAS Collaboration, *Jet energy scale and its systematic uncertainty in proton-proton collisions at* $\sqrt{s} = 7$ *TeV in ATLAS 2010 data*, ATLAS-CONF-2011-032.

[53] TheATLAS Collaboration, *Performance of the Reconstruction and Identification of Hadronic tau Decays in ATLAS with 2011 Data*, ATLAS-CONF-2012-142.

[54] The ATLAS Collaboration, *Reconstruction and Calibration of Missing Transverse Energy and Performance in Z and W events in ATLAS Proton-Proton Collisions at* $\sqrt{s}$*=7 TeV*, ATLAS-CONF-2011-080.

[55] A. Elagin, P. Murat, A. Pranko, and A. Safonov, *A New Mass Reconstruction Technique for Resonances Decaying to di-tau*, `arXiv:1012.4686 [hep-ex]`. * Temporary entry *.

[56] ATLAS Jet/EtMiss Combined Performance Group, *Jet Energy Resolution Provider*, https://twiki.cern.ch/twiki/bin/view/Main/JetEnergyResolutionProvider.

[57] The ATLAS Collaboration, *Data-Quality Requirements and Event Cleaning for Jets and Missing Transverse Energy Reconstruction with the ATLAS Detector in Proton-Proton Collisions at a Center-of-Mass Energy of* $\sqrt{s} = 7$ *TeV*, ATLAS-CONF-2010-038.

[58] T. A. Collaboration, *Search for neutral MSSM Higgs bosons decaying to $\tau\tau$ pairs in proton-proton collisions at with the ATLAS detector*, Physics Letters B **705** (2011) no. 3, 174 – 192.

[59] The ATLAS Collaboration, *Data-driven estimation of the background to charged Higgs boson searches using hadronically-decaying tau final states in ATLAS,* ATLAS-CONF-2011-051.

[60] The ATLAS Collaboration, *Measurement of the $Z \to \tau\tau$ cross section with the ATLAS detector*, Phys. Rev. D **84** (2011) 112006.

[61] T. A. Collaboration, *Search for the neutral Higgs bosons of the Minimal Supersymmetric Standard Model in pp collisions at $\sqrt{s} = 7$ TeV with the ATLAS detector*, JHEP , `arXiv:1211.6956`.

[62] Atlas statistics forum, *ABCD method in searches*, link

[63] The ATLAS Collaboration, *Search for Neutral MSSM Higgs Bosons H to $\tau\tau$ to $l\tau_h$ with the ATLAS Detector in 7 TeV Collisions*, ATL-COM-PHYS-2012-094.

[64] The ATLAS Collaboration, *Search for neutral Higgs Bosons in the decay mode $H \to \tau\tau \to ll{+}4\nu$ in proton proton collision at $\sqrt{7}$ TeV with the ATLAS Detector*, ATL-COM-PHYS-2011-758.

[65] The ATLAS Collaboration, *Measurement of the b-tag Efficiency in a Sample of Jets Containing Muons with 5 fb^{-1} of Data from the ATLAS Detector*, ATLAS-CONF-2012-043.

[66] The ATLAS Collaboration, *Luminosity Determination in pp Collisions at $\sqrt{s} = 7$ TeV using the ATLAS Detector in 2011*, ATLAS-CONF-2011-116.

[67] T. Sjostrand, S. Mrenna and P. Skands, *PYTHIA 6.4 physics and manual*, JHEP **05** (2006) 026.

[68] A. B. et al., *Rivet user manual*, `arXiv:1003.0694 [hep-ph]`.

[69] E. G. G. Cowan, K. Cranmer and O. Vitells, *Asymptotic formulae for likelihood-based tests of new physics*, `arXiv:1007.1727 [hep-ex]`.

[70] LHC Higgs Cross Section Working Group, S. Dittmaier, C. Mariotti, G. Passarino, R. Tanaka (Eds.), et al., *Handbook of LHC Higgs Cross Sections: 1. Inclusive Observables*, `arXiv:1101.0593 [hep-ph]`.

[71] LHC Higgs Cross Section Working Group, S. Dittmaier, C. Mariotti, G. Passarino, and R. Tanaka (Eds.), *Handbook of LHC Higgs Cross Sections: 2. Differential Distributions*, CERN-2012-002 (CERN, Geneva, 2012) , `arXiv:1201.3084 [hep-ph]`.

[72] D. de Florian, G. Ferrera, M. Grazzini and D. Tommasini, *Transverse-momentum resummation: Higgs boson production at the Tevatron and the LHC*, JHEP **1111** (2011) , `arXiv:1109.2109 [hep-ph]`.

[73] Statistical twiki, NuissanceCheck. https://twiki.cern.ch/twiki/bin/view/AtlasProtected/Nuisan

.1 Object Reconstruction, Preselection and Efficiency Corrections

In this section the preselection and reconstruction criteria for the objects used in this analysis are presented. For each object and selection criteria all corrections that have been applied to data and MC are also described. A summary of the preselection on physics objects used in this analysis is reported in Table 1.

.1.1 Electrons

This analysis uses electrons found by the standard electron identification algorithms [44] that pass the `Medium++` criteria. A preselection is applied to the electrons to ensure that the electron cluster has a transverse energy of $E_T > 15GeV$, is within the pseudorapidity range $|\eta| < 2.47$, but is outside of the region $1.37 < |\eta| < 1.52$. The first requirement ensures that the selected electrons are within a range of E_T where the electron reconstruction and trigger efficiencies are well understood. The further requirements ensure that the electron is reconstructed within the acceptance of the ATLAS tracking, but outside of the transition region between the barrel and end-cap calorimeters. In addition, the author is required to be either one or three, to ensure that the electron was reconstructed with either the standard electron algorithm or both the standard and soft electron algorithms, respectively. Finally, to ensure that the electron is not reconstructed within a region of the calorimeter with readout problems, dead or non-nominal high voltage conditions or suffering from high noise, the electron is rejected if the cluster η and ϕ position match a flagged region in the Object Quality maps (OQ maps) [**?**] provided by the egamma Performance group.

For the electrons used in this analysis, the four-vector of the particle is defined using the energy of the electron calorimeter cluster and the direction of the electron track. Selections that involve the electron position in the calorimeter, in this analysis the η and the OQ map selections, are made using a four-vector built entirely from the electron cluster properties. Both the energy scale and resolution of the electrons used in this analysis are corrected, following the recommendations of the EGamma performance group, by using the `egammaAnalysisUtils` package[**?**]. Energy scale corrections are applied to electrons in data, whereas an additional smearing is applied to the electron energy in MC.

In addition to the preselection defined above, isolation criteria are defined to select electrons with little or no activity around them. The calorimetric isolation, E_T(cone) , is calculated as the sum of the transverse energy of the additional topological clusters in the electromagnetic and hadronic calorimeters in a cone of $\Delta R < 0.2$ around an electron[2] . The summed transverse energy is corrected, as a function of the number of primary vertices in the event, to reduce the dependence on pileup. In addition, the track isolation, p_T(cone) , is defined as the scalar sum of the p_t of all additional tracks with $p_t > 1$ GeV in a cone of radius $\Delta R < 0.4$

[2]The ΔR variable is defined by $\Delta R = \sqrt{(\Delta\eta)^2 + (\Delta\phi)^2}$, where $\Delta\eta$ and $\Delta\phi$ correspond to the difference between the pseudorapidities and azimuthal angles of the objects considered, respectively.

around an electron. In this analysis, an electron with $E_T(\text{cone})/p_t < 0.08$ and $p_T(\text{cone})/p_t < 0.06$ is considered isolated.

.1.2 Muons

Muons reconstructed by the STACO algorithm [44] are used in this analysis - those passing the STACO Loose quality criteria are considered at the preselection stage, whereas the more stringent STACO Combined quality criteria are required for the final muon selection. Muons with a transverse momentum $p_t > 10$ GeV and within the pseudorapidity range $|\eta| < 2.5$ are selected. The difference between the z position of the muon track extrapolated to the beam line and the primary vertex z position must be less than 10 mm.

Further quality criteria are placed on the Inner Detector track of the muon candidate to ensure that it is well reconstructed and to reduce the fake rate due to decays of hadrons in flight. These requirements ensure that multiple hits are found on the track in the various layers of the ID, but take into account that dead or uninstrumented regions may be crossed by the muon. Firstly, if the muon passes through a section of the b layer of the Pixel detector that is instrumented and not suffering from detector problems, there should be one or more b layer hits on the track. The sum of the number of hits on the track in the Pixel detector and the number of crossed dead Pixel detector layers should be at least one. The sum of the number of hits within the SCT detector and the number of dead SCT modules crossed should be five or greater. The total number of crossed dead Pixel detector and SCT detector layers should be less than three. When within the angular region $|\eta| < 1.9$, the sum of the TRT hits and outliers on the track must be greater than five and the ratio of TRT outlier hits to the total number of TRT hits must be less than 0.9. When the muon track is in the region $|\eta| \geq 1.9$, the ratio of TRT outlier hits to the total number of TRT hits must be less than 0.9 only if the sum of the TRT hits and outliers on the track is be greater than five.

The momentum scale and resolution of the muons in this analysis are corrected in MC following the recommendations of the Muon Combined Performance group. The momentum corrections were measured by comparing the di-muon mass peak position and resolution between data and MC at the Z resonance. Smearings are applied in a coherent manner to the ID, MS extrapolated and combined momenta of the transverse momentum of the muon. In addition, a scale correction is applied to the combined momentum momentum.

As for the electrons used in this analysis, both calorimeteric and track based isolation are used to require little or no activity around them, in addition to the preselection above. The muon $E_T(\text{cone})$ and $p_T(\text{cone})$ variables are defined as for the electron case and are calculated in cones of $\Delta R < 0.2$ and $\Delta R < 0.4$ around the muon, respectively. Once more $E_T(\text{cone})$ is corrected as a function of the number of primary vertices in the event, to reduce the dependence on pileup. In this analysis, a muon with $E_T(\text{cone})/p_t < 0.04$ and $p_T(\text{cone})/p_t < 0.06$ is considered isolated.

.1.3 Jets

The jets used in this analysis are reconstructed using the Anti-k_T algorithm [49] with the distance parameter R=0.4 taking topological clusters as inputs. The reconstructed jets are calibrated to the Local Cluster Weighting (LCW) scale [**?**]. In addition, the effect of pileup on the reconstructed energy is reduced by applying a further correction based on the pile-up area method with a final in-situ calibration also applied.

A preselection is then applied that requires the reconstructed jets have a transverse momentum, after calibration, of $p_t > 30$ GeV and to be within the pseudorapidity range $|\eta| < 4.5$. The effect of pileup on the reconstructed jets is further reduced by requiring that jets with the pseudorapidity range $|\eta| < 2.4$ and a transverse momentum of $p_t < 50$ GeV have a absolute value of the Jet Vertex Fraction (JVF) of greater than 0.5.

A separate set of preselected jets is defined that are used only for b-tagging (henceforth known as "taggable jets"). Such jets are reconstructed and calibrated as for the standard preselected jets. However, the taggable jets are required to have a transverse momentum of $p_t > 20$ GeV and to have a reconstructed pseudorapidity of $|\eta| < 2.5$. The second requirement ensures that charged particles within the jets pass through the tracking volume and hence can be used for b-tagging of the jet. Finally, the same JVF selection as the standard preselected jets is applied to the taggable jets.

.1.4 b-Tagging

The tagging of jets due to the hadronisation of b-quarks is performed using the MV1 b-tagging algorithm [**?**]. This neural network based algorithm uses the output weights of the JetFitter+IP3D, IP3D and SV1 b-taggers as inputs. The working point that gives a nominal b-tagging efficiency of 70% on $t\bar{t}$ samples is used.

.1.5 Taus

Hadronically decaying tau candidates are reconstructed using clusters in both the electromagnetic and hadronic calorimeters. A preselection is applied to the candidates that requires the reconstructed τ candidates to have a transverse momentum of $p_t > 20$ GeV and to have a reconstructed pseudorapidity of $|\eta| < 2.5$. Furthermore, it is required that the candidates have either one or three tracks within a cone of $\Delta R < 0.2$ associated to them and have a charge of ± 1. Finally, the preselected tau candidates should pass the BDT-Medium multivariant tau identification selection as well as the dedicated electron and muon vetoes for hadronically decaying tau candidates.

.1.6 Overlap Removal

After the preselection of the physics objects needed for this analysis, an overlap removal between the different objects is then applied to avoid double-counting.

The distance between two objects in rapidity $\Delta\eta$ and polar angle $\Delta\phi$ is defined as $\Delta R = \sqrt{(\Delta\eta)^2 + (\Delta\phi)^2}$. Overlap removal is then applied in the following order:

- preselected electrons are removed if they overlap with a preselected muon within $\Delta R < 0.2$,
- preselected taus are removed if they overlap with a preselected muon or electron within $\Delta R < 0.2$,
- preselected jets are removed if they overlap with a preselected muon, electron or tau within $\Delta R < 0.2$.

.1.7 Missing Transverse Energy

The missing transverse energy, E_T^{miss}, is calculated using the RefFinal method, which takes the energy deposited in the calorimeter, the muons reconstructed in the muon spectrometer and tracks reconstructed in the inner detector as inputs. For this, the energy deposits are calibrated based upon the high-p_t physics object they are associated to, with an order of preference of electrons, photons, hadronically decaying taus, jets and finally muons. Any unassociated energy deposits are combined into the so-called "soft-term". To reduce the effect of pileup on the E_T^{miss} calculation, corrections are applied to both the jets in an event and to the soft-term. Firstly, any jet with a pseudorapidity of $|\eta| < 2.4$ that enters the E_T^{miss} calculation is weighted by it's JVF. Similarly, the soft-term is weighted by the soft-term-vertex-fraction (STVF) of the event - the ratio given by

$$STVF = \frac{\sum_{track,PV} p_t}{\sum_{track} p_t} \tag{1}$$

where $\sum_{track,PV} p_t$ is the sum of the transverse momentum of all tracks associated to the primary vertex, but unmatched to physics objects, and $\sum_{track} p_t$ is the sum of the transverse momentum of all tracks in the event unmatched to physics objects. Any calibration applied to the energy or direction of the physics objects in the final analysis is also propagated to the E_T^{miss}.

.1.8 Vertices

In this analysis vertices are selected that have a minimum of three associated tracks: this helps to ensure that the selected vertices come from beam-beam interactions rather than, for instance, cosmic muons.

.1.9 Event Cleaning

In addition to the data quality requirements described in section **??**, further selections are applied to veto events where bad jets are identified as arising from detector effects (coherent noise in the EM and Tile calorimeters or spikes in the

Physics Object	Preselection
Electrons	$p_t > 15$ GeV
	$\|\eta\| < 1.37$ or $1.52 < \|\eta\| < 2.47$
	`Medium++`
	Author = 1 or 3
	Pass Object Quality Flag
Muons	$p_t > 10$ GeV
	$\|\eta\| < 2.5$
	isLoose STACO muon
	Inner Detector track quality requirements
	Inner Detector track $\|z_0^{PV}\| < 10$mm
Jets	$p_t > 30$ GeV
	$\|\eta\| < 4.5$
	$\|JVF\| > 0.5$ for jets with $\|\eta\| < 2.4$ and $p_t < 50$ GeV
Jets (taggable)	$p_t > 20$ GeV
	$\|\eta\| < 2.5$
	$\|JVF\| > 0.5$ for jets with $\|\eta\| < 2.4$ and $p_t < 50$ GeV
Taus	$p_t > 20$ GeV
	$\|\eta\| < 2.5$
	BDT Medium
	$N_{tracks} = 1$or3
	Author = 1 or 3
	Muon and Electron Veto
E_T^{miss}	RefFinal with STVF correction
Vertices	$N_{tracks} \geq 3$

Table 1: Summary of the preselections used for physics objects in this analysis

HEC calorimeter), cosmics or beam based background. To reject events, the recommendations of the JetEtMiss performance group [**?**] are followed: Events are rejected if at least one AntiKt4LCTopo jet with $p_T > 20$ GeV, that passes the overlap removal with electrons, muons and taus described in section .1.6, fails the `BadLooseMinus` selection or points towards the hot Tile Calorimeter cells identified in data taking periods B1 and B2 [**?**].

.1.10 Monte Carlo Corrections

The MC samples used on this analysis are corrected to account for differences between the simulation and data in the trigger, lepton reconstruction and identification and b-tagging efficiencies. Furthermore, the MC is reweighted so that the vertex multiplicity distribution agrees with that in the data.

Trigger Efficiency corrections

Correction factors are applied to the simulated trigger efficiency for both the single electron,
`EF_e24vhi_medium1`, and combined electron-muon, `EF_e12Tvh_medium1_mu8`, triggers used in this analysis. The trigger efficiency for the `EF_e24vhi_medium1` has been measured with respect to offline electrons using a tag and probe method in $Z \to ee$ events [**?**]. Scale factors are derived from the ratio of the trigger efficiency measured in data and MC, measured as a function of electron p_t and η.

For the `EF_e12Tvh_medium1_mu8` trigger, correction factors are measured separately for the two individual legs of the trigger, `EF_e12Tvh_medium1` and `EF_mu8` [**?**]. The product of the two correction factors is then used as the overall scaling factor. The trigger efficiency for the `EF_e12Tvh_medium1` leg has been measured with respect to offline electrons using a tag and probe method for $Z \to ee$ events in both data and MC. Likewise, the `EF_mu8` trigger efficiency scale factors are derived using a tag and probe measurement with $Z \to \mu\mu$ events. Oncemore, scale factors are derived from the ratio of the trigger efficiency measured in data and MC, measured as a function of electron p_t and η.

Lepton Reconstruction Efficiency Corrections

Further correction factors are applied to the MC samples to account for differences in the lepton reconstruction and identification efficiencies between data and simulation. Scale factors for the electron identification and reconstruction efficiencies are measured separately using a combination $Z \to ee$ and $J/\psi \to ee$ tag and probe measurements [**?**]. Both sets of scale factors are measured as a function of the electron E_T and η.

Similarly, muon reconstruction efficiency scale factors have been measured, using a $Z \to \mu\mu$ tag and probe analysis, as a function of the muon p_t, η, ϕ and charge [**?**].

b-tagging Efficiency Corrections

Corrections are applied to the b-tagging efficiency and mistag rate in MC, using a combination of the System8 and likelihood scale factor measurements [**?**]. Separate scale factors are applied based on the origin of the jet at truth level - from a b quark, a c quark, a τ or a light quark - and are applied as a function of the jet p_t and η.

Pileup Reweighting

Differences between the distribution of the average number of interactions per bunch crossing, $< \mu >$, in MC and data are corrected by reweighting the MC $< \mu >$ distribution to that in the full considered dataset. An additional scaling of $1.1\times <$ $\mu >$ is applied to the MC, which has been shown to improve the description of the number of primary vertices distribution of the data.